

Using Causality for Enhanced Prediction of Web Traffic Time Series

Chang Tian
KU Leuven
Leuven, Belgium

Mingzhe Xing
Zhongguancun Laboratory
Beijing, China

Zenglin Shi
Hefei University of Technology
Hefei, China

Matthew B. Blaschko
KU Leuven
Leuven, Belgium

Yinliang Yue
Zhongguancun Laboratory
Beijing, China

Marie-Francine Moens
KU Leuven
Leuven, Belgium

ABSTRACT

Predicting web service traffic has significant social value, as it can be applied to various practical scenarios, including but not limited to dynamic resource scaling, load balancing, system anomaly detection, service-level agreement compliance, and fraud detection. Web service traffic is characterized by frequent and drastic fluctuations over time and are influenced by heterogeneous web user behaviors, making accurate prediction a challenging task. Previous research has extensively explored statistical approaches, and neural networks to mine features from preceding service traffic time series for prediction. However, these methods have largely overlooked the causal relationships between services. Drawing inspiration from causality in ecological systems, we empirically recognize the causal relationships between web services. To leverage these relationships for improved web service traffic prediction, we propose an effective neural network module, CCMPlus, designed to extract causal relationship features across services. This module can be seamlessly integrated with existing time series models to consistently enhance the performance of web service traffic predictions. We theoretically justify that the causal correlation matrix generated by the CCMPlus module captures causal relationships among services. Empirical results on real-world datasets from Microsoft Azure, Alibaba Group, and Ant Group confirm that our method surpasses state-of-the-art approaches in Mean Squared Error (MSE) and Mean Absolute Error (MAE) for predicting service traffic time series. These findings highlight the efficacy of leveraging causal relationships for improved predictions.

1 INTRODUCTION

User-oriented web services continue to grow exponentially, especially with the advancements in artificial intelligence (AI) techniques [25, 36, 40], which have significantly accelerated the development of a diverse range of customized web applications. These services attract a substantial user base and play a pivotal role in enabling various social and practical activities. For instance, YouTube has amassed 2.7 billion users¹, powered by its cutting-edge recommendation algorithms. Accurately predicting web service traffic carries significant social and practical value, with applications spanning dynamic resource scaling [29, 52], load balancing [30], system anomaly detection [26], service-level agreement compliance [23], fraud detection [2], and so on. These capabilities not only enhance

system performance but also improve the overall user experience with these technologies [22].

Co-located, long-running web services often experience diverse workload patterns [52]. Web service traffic are characterized by frequent and significant fluctuations over time, driven by heterogeneous user behaviors at any given moment. These factors collectively make predicting web service traffic a highly challenging task [29, 37]. Previous works conduct extensive research to predict the web service traffic, often formulating it as a typical time series forecasting task. These approaches can broadly be categorized into statistical [14, 20, 21], machine learning [6, 15, 17], and deep learning [11, 29, 34, 52] methods. While statistical methods struggle to handle multi-dimensional and non-linear traffic data, machine learning methods address these limitations but fail to achieve the same level of accuracy as deep learning approaches. Among the deep learning based methods, the recent advancements in Transformer [42] architecture have demonstrated superior performance in sequential prediction tasks. Consequently, Transformer-based methods have emerged, achieving promising results [32] in web service traffic prediction. However, they did not pay enough attention to the causal relationship across web services.

In addition to the three types of specialized methods previously discussed for predicting web service traffic, general time series forecasting methods are also widely employed in practice [3, 52]. These approaches are typically divided into two categories [33]: statistical methods and neural network-based methods. Since statistical methods often fail to capture complex temporal features, neural network-based methods generally achieve superior performance [47]. Neural network-based approaches can be further classified into five paradigms [39, 44]: Recurrent neural network (RNN)-based, convolutional neural network (CNN)-based, Transformer-based, multi-layer perceptron (MLP)-based, and large language model (LLM)-based methods. CNN-based methods [13, 43] use convolutional kernels along the temporal dimension to identify sequential patterns, whereas RNN-based methods [9, 10, 31] rely on recurrent structures to model temporal state transitions. Transformer-based methods [5, 24, 46, 51] are widely recognized for their ability to effectively extract features using attention mechanisms. LLM-based methods [19, 39, 41] leverage advanced reasoning capabilities by processing time series data through specially designed prompts, offering a promising avenue for temporal modeling. Finally, MLP-based methods [7, 27, 46, 47] strike a compelling balance between forecasting accuracy and computational efficiency. It is regrettable that when advanced general time series forecasting methods are

¹<https://www.globalmediainsight.com/blog/youtube-users-statistics/>

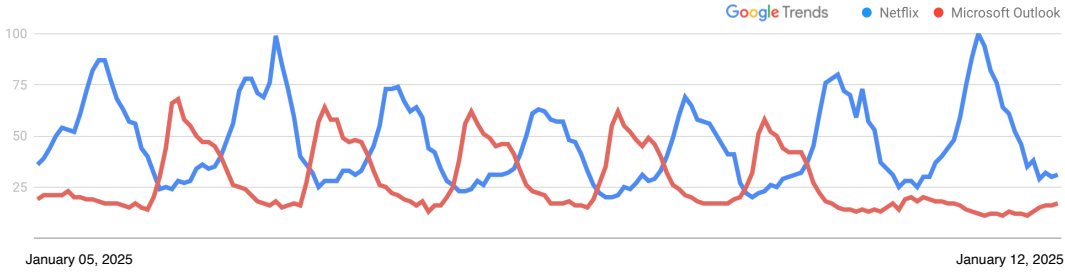


Figure 1: This figure illustrates 7-day search interest data for Netflix and Microsoft Outlook from Google Trends. The vertical axis represents normalized search interest as a percentage relative to the highest point on the chart for the specified time period. The horizontal axis corresponds to the time period from January 5th, 2025 to January 12th, 2025.

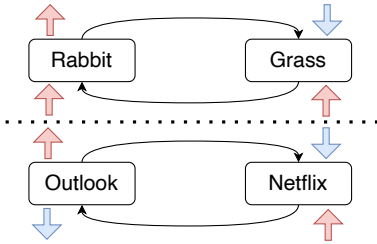


Figure 2: Illustration of ecological and analogical web service causality. The rabbit population influences grass abundance [18], where an increase in rabbits leads to a decrease in grass. This principle inspires our CCMPPlus module, which captures causal effects among web services.

applied to web traffic prediction, the causal relationships among services are not utilized.

Drawing inspiration from ecological causality, as illustrated in Figure 2, where grass abundance and rabbit populations influence one another iteratively [18], we identify analogous patterns in web service traffic as shown in Figure 1. Empirical observations of Google Trends data reveal a causal relationship between leisure websites, such as Netflix, and work-related software, like Outlook. Specifically, increased web traffic to Netflix corresponds to decreased traffic to Outlook, and vice versa. These empirical observations suggest the existence of latent causal relationships underlying human-driven web behaviors. By uncovering and leveraging these causal relationships, we can achieve more accurate modeling of service traffic patterns. Building on this motivation and the causality theory of Convergent Cross Mapping (CCM) [38], which originates from ecology, we introduce the CCMPPlus module. This module extracts features from web service traffic time series while including causal relationships among services, thereby enhancing the accuracy of web service traffic prediction. Furthermore, the CCMPPlus module could integrate easily with existing time series forecasting models, enriching them with more informative, causally-aware features.

Concretely, we extend the CCM theory to effectively merge with neural networks, resulting in the development of the CCMPPlus

module. The CCMPPlus module operates in three key steps: first, it extracts initial feature representations from web service traffic time series; second, it computes a causal correlation matrix from a multi-manifold space based on these feature representations; and finally, it applies the causal correlation matrix to the initial feature representations, generating a resulting feature representation that incorporates informative causal information. This enhanced feature representation can then be concatenated with the feature representations of web service traffic time series extracted by existing time series models, thereby improving prediction accuracy.

Our main contributions in this work can be summarized as follows:

- **Method:** The CCMPPlus module enhances existing time series forecasting models by generating feature representations that incorporate causal relationships across web services, addressing a critical limitation of many previous methods. Additionally, the CCMPPlus module is designed for seamless integration with existing time series forecasting models, further contributing to improved prediction accuracy.
- **Theory:** We justify that the causal correlation matrix generated by the CCMPPlus module effectively captures causal relationships across web services, enabling the incorporation of these relationships into web traffic prediction methods.
- **Experiments:** Experiments conducted on three real-world web service traffic datasets (Alibaba Group, Microsoft Azure, and Ant Group) demonstrate that our method achieves superior performance in terms of Mean Squared Error (MSE) and Mean Absolute Error (MAE) compared to previous state-of-the-art (SOTA) methods, thereby validating the effectiveness of the CCMPPlus module.

The remainder of the paper is organized as follows. Section 2 reviews related work. Section 3 provides preliminary information about our proposed method. Section 4 elaborates on the proposed framework, encompassing the CCMPPlus and time series backbone modules. Section 5 compares experimental results from the proposed method and prevalent methods, and analyzes the method and results. Section 6 concludes this paper.

2 RELATED WORK

2.1 Web Service Traffic Prediction

Web service traffic prediction is a task critical to enabling service autoscaling, load balancing, and anomaly detection. As web service traffic is often represented as time series data, existing approaches primarily frame traffic prediction as a time series prediction problem [3, 29, 52].

Early research focused on statistical prediction methods [14, 20, 21] such as Moving Average, Auto-Regression, and Autoregressive Integrated Moving Average. These methods are valued for their simplicity and interpretability but are constrained by strict stationarity requirements. Moreover, they struggle to extend to multi-dimensional or non-linear data, limiting their applicability in dynamic environments. To overcome these limitations, methods like HOPBLR [17], LLR [6] and TWRES [15] employed machine learning techniques, including Logistic Regression and Support Vector Regression, respectively, for traffic prediction. However, these approaches were hindered by the limited expressive capacity of their models, resulting in suboptimal prediction accuracy. More recent advancements have shifted towards deep learning methods. CrystallLP [34] and GRUWP [11] utilize Long Short-Term Memory networks and Gated Recurrent Units, respectively, to predict service workloads. MagicScaler [29] proposes a novel multi-scale attentive Gaussian process-based predictor, capable of accurately forecasting future demands by capturing scale-sensitive temporal dependencies. The Performer [32] integrates the Transformer architecture into an encoder-decoder paradigm for service workload prediction. It leverages the self-attention mechanism to model temporal correlations and learn both global and local representations effectively. OptScaler [52] advances this direction with a proactive prediction module comprising a long-term periodic block and a short-term local block to capture multi-scale temporal dependencies. While existing traffic prediction methods demonstrate high accuracy through advanced time series forecasting techniques, they largely neglect the underlying causal relationships within the web services. Exploring these hidden causalities holds significant potential for further improving prediction performance.

2.2 Time Series Forecasting

Besides approaches specifically tailored for web service traffic prediction, general time series forecasting methods are also applied to predict web traffic [3, 8, 52].

Traditional statistical methods such as Prophet [35], and Holt-Winters [16] assume that time series variations adhere to predefined patterns. However, the inherently complex fluctuations of web service traffic often exceed the scope of these predefined patterns, thereby limiting the practical applicability of such statistical methods [47].

Recent advancements in neural network architectures have significantly enhanced temporal modeling capabilities. Neural network approaches for time series forecasting can be categorized into five paradigms [39, 44]: RNN-based, CNN-based, Transformer-based, MLP-based, and large language model (LLM)-based methods.

Empirical methods often integrate components from the aforementioned categories, utilizing specific designs to effectively capture critical temporal features [44]. These specific designs incorporate series decomposition, multi-periodicity analysis, and multi-scale mixing architectures.

For series decomposition, Autoformer [48] introduces a decomposition block based on moving averages, enabling the separation of complex temporal variations into seasonal and trend components. Building on this foundation, DLinear [49] utilizes series decomposition as a preprocessing step prior to performing linear regression. Crossformer [50] segments time series data into subseries-level patches and employs a Two-Stage Attention layer to effectively model cross-time and cross-variable dependencies within each patch. iTransformer [24] leverages the global representation of entire series and applies attention mechanisms to these series-wise representations, facilitating the capture of multivariate correlations. TimeXer [46] integrates external information into the Transformer architecture through a carefully designed embedding strategy, allowing the inclusion of external information into patch-wise representations of endogenous series. In the context of multi-periodicity, NBEATS [28] employs multiple trigonometric basis functions to model time series, providing a robust framework for handling periodic patterns. Similarly, TimesNet [47] applies Fourier Transform to decompose time series into components of varying periodic lengths and utilizes a modular architecture to process these decomposed components effectively. With respect to multi-scale mixing architectures, Pathformer [5] adopts multi-scale patch representations and applies dual attention mechanisms across these patches to capture both global correlations and local details, thereby addressing temporal dependencies comprehensively. TimeMixer [44] captures temporal features by introducing a novel multi-scale mixing architecture, which comprises two key components: Past-Decomposable-Mixing, designed to leverage disentangled series for multi-scale representation learning, and Future-Multipredictor-Mixing, which ensembles complementary forecasting skills across multi-scale series to enhance prediction accuracy.

While general time series forecasting methods have been applied to web service traffic prediction [4, 29, 52], these methods often overlook causal relationships between services. In contrast, our CCMPlus module computes a causal correlation matrix used to generate temporal features incorporating causal relationships, significantly improving web service traffic prediction accuracy.

3 PRELIMINARIES

In this section, we begin by presenting the time series patterns observed in web service traffic, illustrated with a specific web service traffic example. Subsequently, we provide an overview of the ecological causality theory, Convergent Cross Mapping (CCM) [38], which serves as the theoretical foundation for our proposed CCM-Plus module for web service traffic prediction.

3.1 Web Service Traffic

Figure 3 presents an illustrative example of web service traffic time series from Microsoft Azure. It exhibits significant fluctuations and frequent changes, primarily driven by human behavior and

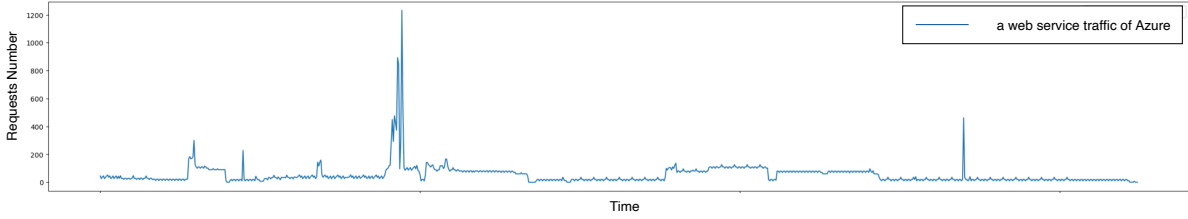


Figure 3: Web service traffic time series from the Microsoft Azure cluster. The horizontal axis represents time progression, while the vertical axis indicates the number of service requests at each time point.

activity patterns. The web traffic prediction task can be formulated as follows:

$$y(t) = P(y(t - \alpha), y(t - 2\alpha), \dots, y(t - k\alpha)),$$

where $y(t)$ is the number of request at time t , α denotes the prediction granularity, and k is the historical sequence length. However, accurately predicting web service traffic remains a well-recognized challenge due to the inherent complexity of traffic patterns, as highlighted by the research community [29, 52].

3.2 Convergent Cross Mapping

Convergent Cross Mapping (CCM) theory published in Science [38] was originally proposed in the field of ecology and is designed to detect causal relationships between species. The exposition of CCM is often illustrated using the context of the Lorenz system, as depicted in Figure 4.

As depicted in Figure 4, the trajectory of the Lorenz system forms a manifold M in the state space. This manifold M consists of a collection of points that represent all possible states of the Lorenz system over time, with these points connected to create a structured geometric space. The manifold, also referred to as the attractor, encompasses all trajectories and potential states $\underline{m}(t)$ of the system. Each state $\underline{m}(t)$ corresponds to a point in M , represented by the coordinate vector $\underline{m}(t) = [X(t), Y(t), Z(t)]$.

The shadow manifold, M_x or M_y , represents the projection of the original manifold M onto the system variables X or Y , respectively. Specifically, a lagged coordinate embedding utilizes E time-lagged values of $X(t)$ as coordinate axes to reconstruct the shadow manifold M_x . A point on M_x , denoted as $\underline{x}(t)$, is an E -dimensional vector expressed as:

$$\underline{x}(t) = [X(t), X(t - \tau), X(t - 2\tau), \dots, X(t - (E - 1)\tau)],$$

where τ is a positive time lag, and E denotes the embedding dimension. In Figure 4, $E = 3$. Similarly, the same approach applies to points $\underline{y}(t)$ in the manifold M_y , defined as:

$$\underline{y}(t) = [Y(t), Y(t - \tau), Y(t - 2\tau), \dots, Y(t - (E - 1)\tau)].$$

3.2.1 Cross Mapping. Cross mapping refers to the process of identifying contemporaneous points in the manifold M_x of one variable X based on points in the manifold M_y of another variable Y . Specifically, given a point $\underline{y}(t)$ in the manifold M_y , the corresponding point in time from the manifold M_x is $\underline{x}(t)$.

As illustrated in Figure 5, if Y exerts a causal effect on X , information from Y will be stored in X . Consequently, the neighbors of

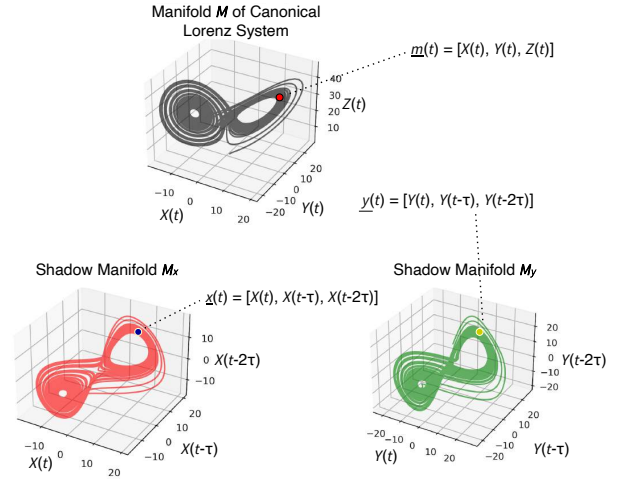


Figure 4: The Convergent Cross Mapping (CCM) theory is often explained using the Lorenz system, utilizing its original manifold and corresponding shadow manifolds.

$\underline{x}(t)$ in M_x will correspond to points with the same time indices in M_y , and these corresponding points will also be neighbors of $\underline{y}(t)$. However, as noted in [38], if Y has no causal effect on X , the information about Y in X will be incomplete. As a result, the timely corresponding points in M_y will diverge and no longer be neighbors of $\underline{y}(t)$.

3.2.2 Convergence. Convergence in CCM implies that if the variable Y has a causal effect on X , extending the observation period improves the ability to predict Y using points on the shadow manifold M_x , as illustrated in Figure 6. A longer observation period provides more trajectories to fill the gaps in the manifold, resulting in a more defined structure, which enhances the prediction of $\hat{Y}(t) | M_x$. Conversely, if two variables do not have a causal relationship, refining their manifolds will not lead to an improvement in predictive accuracy.

3.2.3 CCM Procedure. The CCM procedure for detecting whether variable Y has causal effects on X consists of four key steps:

- **Step 1: Construct the shadow manifold M_x .** Consider two time-evolving variables $X(k)$ and $Y(k)$ of length L , where the time index k ranges from 1 to L . The shadow

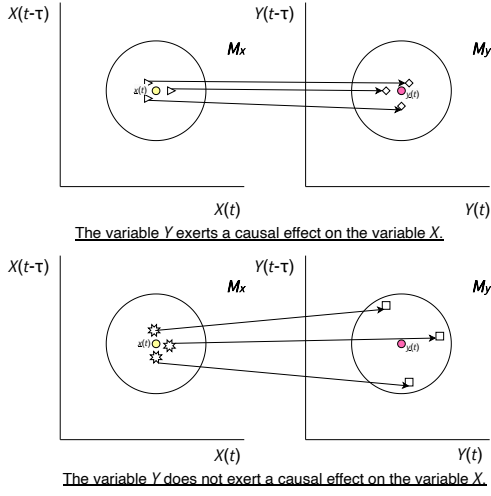


Figure 5: Cross mapping. The point $\underline{y}(t)$ in the manifold M_y corresponds to the contemporaneous point in time $\underline{x}(t)$ in the manifold M_x .

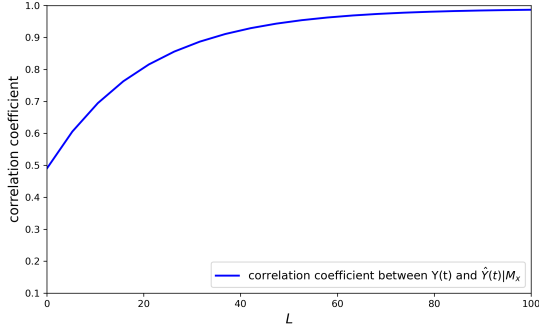


Figure 6: Convergent predictability as the time series length increases, assuming Y has a causal effect on X .

manifold M_x is constructed by forming lagged coordinate vectors:

$$\underline{x}(t) = [X(t), X(t - \tau), X(t - 2\tau), \dots, X(t - (E - 1)\tau)],$$

for $t = 1 + (E - 1)\tau$ to $t = L$. Here, τ represents the time lag, and E denotes the embedding dimension.

- **Step 2: Identify nearest neighbors in M_x .** To estimate $Y(t)$ for a specific t in the range $1 + (E - 1)\tau$ to L , use the shadow manifold M_x . Denote the estimated value as $\hat{Y}(t) | M_x$. Begin by locating the contemporaneous lagged coordinate vector $\underline{x}(t)$ in M_x , and find its $E + 1$ nearest neighbors. Note that $E + 1$ is the minimum number of points needed for a bounding simplex in an E -dimensional space. Let the time indices of these neighbors (ranked by proximity) be t_1, t_2, \dots, t_{E+1} . The nearest neighbors of $\underline{x}(t)$ in M_x are therefore denoted by $\underline{x}(t_i)$, where $i = 1, \dots, E + 1$.

- **Step 3: Estimate $Y(t)$ using locally weighted means.** The time indices t_1, t_2, \dots, t_{E+1} corresponding to the nearest neighbors of $\underline{x}(t)$ are used to identify points in the variable $Y(k)$. These points are then used to estimate $Y(t)$ through a locally weighted mean of the $E + 1$ values $Y(t_i)$:

$$\hat{Y}(t) | M_x = \sum_{i=1}^{E+1} w_i Y(t_i),$$

where w_i represents the weight based on the distance between $\underline{x}(t)$ and its i -th nearest neighbor in M_x , and $Y(t_i)$ are the contemporaneous values of variable $Y(k)$. The weights w_i are determined by:

$$w_i = \frac{u_i}{\sum_{j=1}^{E+1} u_j},$$

where

$$u_i = \exp \left\{ -\frac{d[\underline{x}(t), \underline{x}(t_i)]}{d[\underline{x}(t), \underline{x}(t_1)]} \right\}.$$

Here, $d[\underline{x}(t), \underline{x}(t_i)]$ denotes the Euclidean distance between the two vectors.

- **Step 4: Calculate the correlation coefficient r .** Finally, calculate the correlation coefficient r between $\hat{Y}(t)$ and $Y(t)$, where t ranges from $1 + (E - 1)\tau$ to L :

$$r = \frac{\sum_{t=1+(E-1)\tau}^L (Y(t) - \bar{Y}(t)) (\hat{Y}(t) - \bar{\hat{Y}}(t))}{\sqrt{\sum_{t=1+(E-1)\tau}^L (Y(t) - \bar{Y}(t))^2 \sum_{t=1+(E-1)\tau}^L (\hat{Y}(t) - \bar{\hat{Y}}(t))^2}}.$$

If variable Y has causal effects on X , $\hat{Y}(t)$ will converge to $Y(t)$ as the observation period increases. In ideal cases, the correlation coefficient r will approach 1.

4 METHODOLOGY

Inspired by the concept of causal relationships in ecology, as illustrated in Figure 2, the population dynamics of rabbits influence the abundance of grass—for instance, a higher rabbit population leads to reduced grass availability. Similarly, we observe causal relationships in the web traffic patterns of different web services, as depicted in Figure 1. For example, real-world data from Google Trends indicates that an increase in web traffic for Netflix corresponds to a decrease in traffic for the office software Outlook.

To leverage the latent causality between services for traffic prediction, we extend the ecology CCM theory by integrating into a neural module, referred to as CCMPPlus (CCM+). As illustrated in Figure 7, the CCMPPlus module leverages causal relationships among web services to generate the CCMPPlus representation (Section 4.1). This representation is then concatenated with the representation produced by the Backbone Time Series Model (Section 4.2), to enhance the accuracy of web service traffic time series prediction. Finally, we introduce the optimization process in section 4.3.

4.1 CCMPPlus Module

In this section, we aim to derive a feature representation that captures causal relationships across web services from raw time series data, thereby improving the precision of traffic prediction. This process involves constructing the causal correlation matrix by estimating each time point of one web service time series using points

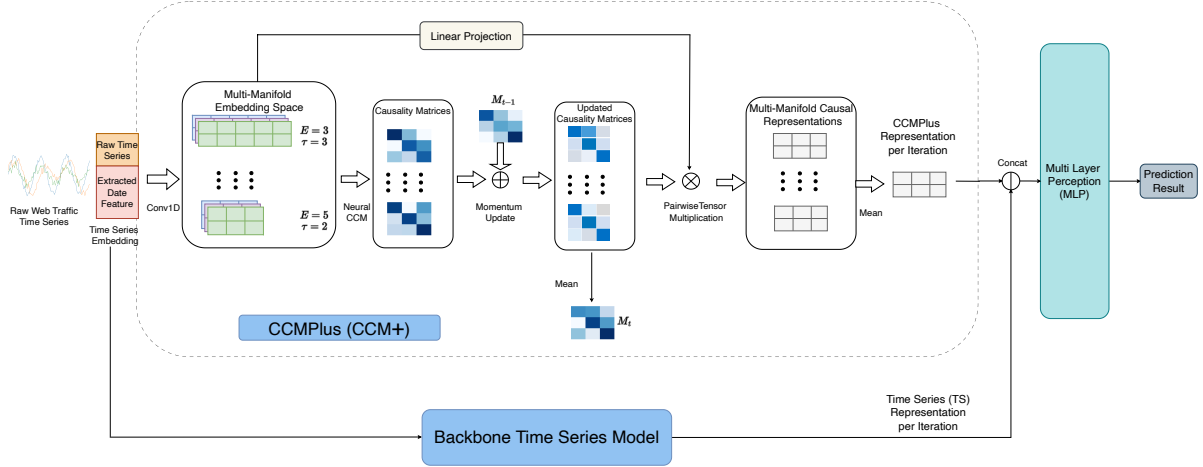


Figure 7: An overview of the proposed method, which consists of two components: the CCMPlus module and the Backbone Time Series Model. The CCMPlus module identifies causal relationships among web services, generating a CCMPlus representation that enhances the predictive performance of the Backbone Time Series Model. Per iteration refers to the entire method’s operations on a single batch of data.

from the shadow manifolds of another web service time series, and then generating the CCMPlus representation using the causal correlation matrix.

The first step is to derive the initial time series embedding. Given the raw time series $\hat{X} \in \mathbb{R}^{B \times N \times L_x}$. Note that for constructing the shadow manifold, the order of \hat{X} along the L_x dimension is reversed. We first extract date features, e.g., minutes, hours and days, and then combine them with the raw time series \hat{X} to form the time series embedding $X \in \mathbb{R}^{B \times N \times L_x \times C_{in}}$. Here, L_x represents the input time series length, and C_{in} denotes the representation dimension of the input.

Next, we employ 1D convolution to construct shadow manifolds for each web service traffic time series. Traditional CCM algorithm relies expert to set the value of τ , which might introduce human bias. To alleviate this issue, we extend it to a multi-manifold space, so as to learn the causality from diverse shadow manifold spaces. Specifically, we initialize two vectors of $\tau = [\tau_1, \dots, \tau_i, \dots, \tau_n]$ and the corresponding $E = [E_1, \dots, E_i, \dots, E_n]$. For simplicity, we use the i -th shadow manifold, defined by the pair (τ_i, E_i) , as a representative example to explain the subsequent procedures. The steps for other shadow manifolds differ only in the index i . The initialized time lag τ_i and the corresponding embedding dimension E_i are generated as follows:

$$E_i = \begin{cases} \left\lfloor \frac{\tau_w}{\tau_i} \right\rfloor - 1, & \text{if } \left\lfloor \frac{\tau_w}{\tau_i} \right\rfloor \bmod 2 = 0, \\ \left\lfloor \frac{\tau_w}{\tau_i} \right\rfloor, & \text{if } \left\lfloor \frac{\tau_w}{\tau_i} \right\rfloor \bmod 2 = 1, \end{cases}$$

where τ_w is set to 100 based on prior empirical observations for shadow manifolds as established in the literature [1]. The convolution output can be derived as follows:

$$X_{conv} = \text{Conv1D}(\hat{X}; \text{kernel_size} = E_i, \text{dilation} = \tau_i),$$

where $\hat{X} \in \mathbb{R}^{B \times N \times C_{in} \times L_x}$ is reshaped from X , the channels of input and output of Conv1D are C_{in} and C_{out} , respectively. The trajectory

length of the i -th shadow manifold is: $L_{out} = L_x - \tau_i(E_i - 1)$, which aligns with CCM theory Step 1 in Section 3.2.3.

After obtaining the convolution output, we can derive the shadow manifold embedding $X_{ccm} \in \mathbb{R}^{B \times N \times L_{out} \times C_{out}}$ reshaped from X_{conv} , where, for each time point in L_{out} , the corresponding point in the shadow manifold is represented by coordinates in the C_{out} dimension. To ensure consistency with the trajectory length L_{out} of the shadow manifolds across different time series, we define the prediction target as $Y = \hat{X}[:, :, L_{out}]$, where $Y \in \mathbb{R}^{B \times N \times L_{out}}$.

4.1.1 Training Mode. Based on Y and X_{ccm} , we use the points in the shadow manifold of one web service time series to predict the values of another web service time series. The predictions are then compared with the ground truth values of the target web service time series to compute the correlation coefficient for each pair. As a result, we can obtain the causal correlation matrix: $M_{train} \in \mathbb{R}^{B \times N \times N}$, where each element represents the causal relationship between a pair of web services. This procedure corresponds to Steps 2–4 in Section 3.2.3.

The causal correlation matrix M_{train} can be efficiently computed using matrix operations on a GPU, as outlined in Algorithm 1 line 18-25. To illustrate, we use a specific element of M_{train} indexed as (l, m, n) to demonstrate the process for quantifying causal relationships. The value $M_{train}[l, m, n]$ quantifies the causal effect of the service time series $Y[l, n, :]$ (denoted with $y(k)$) on $Y[l, m, :]$ (denoted with $x(k)$).

$P = X_{ccm}[l, m, :, :]$, with $P \in \mathbb{R}^{L_{out} \times C_{out}}$, represents the points on the shadow manifold M_x , where the coordinates of the k -th point are given by $\underline{x}(k) = P[k, :]$. The estimation of web service time series $y(k)$ using the shadow manifold M_x of $x(k)$ is denoted by $\hat{y}(k) | M_x$.

First, we begin by locating the contemporaneous point on M_x , $\underline{x}(k)$, and find its $C_{out} + 1$ nearest neighbors. Next, denote the time indices (from closest to farthest) of the nearest neighbors of

Algorithm 1 Algorithmic Procedure for the CCMPlus Module

Require: $\tau = [\tau_1, \dots, \tau_n]$: list of time lagged parameters, τ_w : time window length, L_x : input time series length, N : the number of web service within the input, C_{in} : the number of input channels for Conv1D, C_{out} : the number of output channels of the Conv1D, $\hat{X} \in \mathbb{R}^{B \times N \times L_x}$: a batch of ground truth time series, $X \in \mathbb{R}^{B \times N \times L_x \times C_{in}}$: a batch of input time series embedding, $M_{cc} \in \mathbb{R}^{N \times N}$: causal correlation matrix, m : the momentum value used for updating the causal correlation matrix across iterations, constrained within the range (0, 1), $num_iterations$: the number of overall iterations, $model_training_flag \in \{True, False\}$: training or inference mode.

Ensure: Output h_{ccm}^{iter} and M_{cc}^{iter}

Step 1: Compute E from τ and τ_w .

```

1: Initialize E as an empty list.
2: for each  $\tau_i$  in  $\tau$  do
3:   Compute  $E_i \leftarrow \left\lfloor \frac{\tau_w}{\tau_i} \right\rfloor$ 
4:   if  $E_i$  is even then
5:      $E_i \leftarrow E_i - 1$ 
6:   end if
7:   Append  $E_i$  to E
8: end for
Step 2: calculate the  $M_{cc}^{iter}$  and  $h_{ccm}^{iter}$ .
9: for  $iter \leftarrow 0, \dots, num\_iterations - 1$  do
10:  multi_space_representations = [], multi_space_corrs = []
11:  for  $i \leftarrow 1 \dots n$  do
12:     $\tau_i \leftarrow \tau[i - 1]$ ,  $E_i \leftarrow E[i - 1]$ 
13:    if  $(L_x - \tau_i \times (E_i - 1)) < 0$  then
14:      continue ▷ Skip if sequence too short
15:    end if
16:    Reverse the order of both X and  $\hat{X}$  along the  $L_x$  dimension. Then reshape X to  $\tilde{X} \in \mathbb{R}^{B \cdot N \times C_{in} \times L_x}$ 
17:     $X_{conv} = \text{Conv1D}(\tilde{X}; \text{kernel\_size} = E_i, \text{dilation} = \tau_i)$ ,  $X_{conv} \in \mathbb{R}^{B \cdot N \times C_{out} \times L_{out}}$ 
18:    if  $model\_training\_flag = True$  then
19:      reshape  $X_{conv}$  to  $X_{ccm} \in \mathbb{R}^{B \times N \times L_{out} \times C_{out}}$ ,  $Y \leftarrow \hat{X}[:, :, : L_{out}]$ 
20:       $dist\_matrix \leftarrow \text{PairwiseDistances}(X_{ccm}, X_{ccm})$ ,  $nearest\_indices \leftarrow \text{argsort}(dist\_matrix, \text{dim} = -1)$ 
21:       $nearest\_indices \leftarrow nearest\_indices[:, :, :, 1 : (C_{out} + 2)]$ 
22:       $nearest\_distances \leftarrow \text{Gather}(dist\_matrix, nearest\_indices)$ 
23:       $u_z \leftarrow \exp\left(-\frac{nearest\_distances}{nearest\_distances[:, :, :, 0:1] + \epsilon}\right)$ ,  $w_z \leftarrow \frac{u_z}{\sum(u_z) + \epsilon}$ 
24:       $Y_{nearest} \leftarrow \text{GatherTargets}(Y, nearest\_indices)$ ,  $\hat{Y} \leftarrow \sum(w_z \times Y_{nearest})$ 
25:       $corr \leftarrow \frac{\text{Cov}(\hat{Y}, Y)}{\sigma(\hat{Y}) \sigma(Y) + \epsilon}$ ,  $M_{train} \leftarrow corr^\top$ 
26:      if  $iter > 0$  then
27:         $M_{train}^{iter} \leftarrow m * M_{train}^{iter-1} + (1 - m) * M_{train}$ 
28:      else
29:         $M_{train}^{iter} \leftarrow M_{train}$ 
30:      end if
31:       $\widehat{M}_{train} \leftarrow \text{Softmax}(M_{train}^{iter}, \text{dim} = -1)$ ,  $M_{cc}^{iter}(i) \leftarrow \text{Mean}(\widehat{M}_{train}, \text{dim} = 0)$ 
32:    else
33:       $M_{test} \leftarrow \text{Repeat}(M_{cc}, B)$ ,  $\widehat{M}_{train} \leftarrow \text{Softmax}(M_{test}, \text{dim} = -1)$ ,  $M_{cc}^{iter}(i) \leftarrow M_{cc}$ 
34:    end if
35:     $conv\_out\_proj \leftarrow \text{LinearProjection}(X_{conv})$ ,  $\widehat{X}_{ccm} \leftarrow \text{Reshape}(conv\_out\_proj, [B, N, C_{out}])$ 
36:     $h_{ccm}^{iter}(i) \leftarrow \widehat{M}_{train} \times \widehat{X}_{ccm}$ 
37:    append  $h_{ccm}^{iter}(i)$  to multi_space_representations, append  $M_{cc}^{iter}(i)$  to multi_space_corrs
38:  end for
39:   $h_{ccm}^{iter} \leftarrow \text{Mean}(\text{Stack}(\text{multi\_space\_representations}), \text{dim} = 0)$ 
40:   $M_{cc}^{iter} \leftarrow \text{Mean}(\text{Stack}(\text{multi\_space\_corrs}), \text{dim} = 0)$ 
41: end for

```

$\underline{x}(k)$ by $t_1, \dots, t_{C_{out}+1}$. These time indices corresponding to nearest neighbors to $\underline{x}(k)$ on M_x are used to identify points in time series y

to estimate $y(k)$ from a locally weighted mean of the $y(t_i)$ values:

$$\hat{y}(k) | M_x = \sum_{i=1}^{C_{out}+1} w_i y(t_i),$$

where w_i represents the weight based on the distance between $\underline{x}(k)$ and its i -th nearest neighbor in M_x , and $y(t_i)$ are the contemporaneous values of time series $y(k)$. The weights w_i are determined by:

$$w_i = \frac{u_i}{\sum_{j=1}^{C_{out}+1} u_j},$$

where

$$u_i = \exp \left\{ -\frac{d[\underline{x}(k), \underline{x}(t_i)]}{d[\underline{x}(k), \underline{x}(t_1)]} \right\}.$$

Here, $d[\underline{x}(k), \underline{x}(t_i)]$ denotes the Euclidean distance between the two points on the shadow manifold M_x .

Finally, we calculate the correlation coefficient $\mathbf{M}_{train}[l, m, n]$ between $\hat{y}(k)$ and $y(k)$, where k ranges from 0 to L_{out} :

$$\mathbf{M}_{train}[l, m, n] = \frac{\sum_{t=0}^{L_{out}} (y(k) - \bar{y}(k)) (\hat{y}(k) - \bar{\hat{y}}(k))}{\sqrt{\sum_{t=0}^{L_{out}} (y(k) - \bar{y}(k))^2 \sum_{t=0}^{L_{out}} (\hat{y}(k) - \bar{\hat{y}}(k))^2}}.$$

To ensure consistent and stable representations, the \mathbf{M}_{train} matrix is updated using a momentum-based approach [12] with the causal correlation matrix from the previous iteration, denoted as $\mathbf{M}_{cc}^{iter-1} \in \mathbb{R}^{N \times N}$, followed by a softmax operation for normalization:

$$\mathbf{M}_{train}^{iter} = (1 - m) \cdot \mathbf{M}_{train} + m \cdot \text{Repeat}(\mathbf{M}_{cc}^{iter-1}, \text{dim} = 0), \quad (1)$$

$$\mathbf{M}_{cc}^{iter}(i) = \text{Mean}(\text{Softmax}(\mathbf{M}_{train}^{iter}, \text{dim} = -1), \text{dim} = 0),$$

where $iter$ denotes the current iteration number, Repeat expands \mathbf{M}_{cc}^{iter-1} into $\mathbb{R}^{B \times N \times N}$, m is the momentum value in the range $(0, 1)$, $\mathbf{M}_{cc}^{iter}(i) \in \mathbb{R}^{N \times N}$ corresponds to the i -th shadow manifold of each web service time series, effectively capturing the causal relationships among the N web services.

The next step is to compute the feature representation $h_{ccm}^{iter}(i)$ incorporating the causal relationships among web services for the i -th shadow manifold. We first transpose the last two dimension of the manifold embedding $\mathbf{X}_{ccm} \in \mathbb{R}^{B \times N \times L_{out} \times C_{out}}$. A linear layer is then applied to reduce the dimension L_{out} to 1. This process produces an intermediate value, denoted as $\widehat{\mathbf{X}}_{ccm} \in \mathbb{R}^{B \times N \times C_{out}}$:

$$\widehat{\mathbf{X}}_{ccm} = \text{LinearLayer}(\text{Transpose}(\mathbf{X}_{ccm})). \quad (2)$$

Then,

$$\begin{aligned} \widehat{\mathbf{M}}_{train} &= \text{Softmax}(\mathbf{M}_{train}^{iter}, \text{dim} = -1), \\ h_{ccm}^{iter}(i) &= \widehat{\mathbf{M}}_{train} \cdot \widehat{\mathbf{X}}_{ccm}, \end{aligned} \quad (3)$$

where $h_{ccm}^{iter}(i) \in \mathbb{R}^{B \times N \times C_{out}}$ is the feature representation derived from the i -th shadow manifold. During each training iteration, the CCPlus representation $h_{ccm}^{iter} \in \mathbb{R}^{B \times N \times C_{out}}$ and causal correlation matrix $\mathbf{M}_{cc}^{iter} \in \mathbb{R}^{N \times N}$ are computed by averaging the representations and matrices from all shadow manifolds:

$$\begin{aligned} h_{ccm}^{iter} &= \text{Mean} \left(\sum_{i=1}^n h_{ccm}^{iter}(i) \right), \\ \mathbf{M}_{cc}^{iter} &= \text{Mean} \left(\sum_{i=1}^n \mathbf{M}_{cc}^{iter}(i) \right), \end{aligned} \quad (4)$$

where $\mathbf{M}_{cc}^{iter}(i) \in \mathbb{R}^{N \times N}$ and $h_{ccm}^{iter}(i) \in \mathbb{R}^{B \times N \times C_{out}}$ are the causal correlation matrix and feature representation for the i -th manifold space, respectively.

4.1.2 Testing Mode. Given $\mathbf{M}_{cc} \in \mathbb{R}^{N \times N}$ from the output of the training stage, it is expanded along the batch dimension to obtain $\mathbf{M}_{test} \in \mathbb{R}^{B \times N \times N}$. A softmax normalization is then applied along the last dimension to produce $\widehat{\mathbf{M}}_{train} \in \mathbb{R}^{B \times N \times N}$:

$$\mathbf{M}_{test} = \text{Repeat}(\mathbf{M}_{cc}, \text{dim} = 0),$$

$$\widehat{\mathbf{M}}_{train} = \text{Softmax}(\mathbf{M}_{test}, \text{dim} = -1).$$

Based on $\mathbf{X}_{ccm} \in \mathbb{R}^{B \times N \times L_{out} \times C_{out}}$ generated by the trained model, $\widehat{\mathbf{X}}_{ccm} \in \mathbb{R}^{B \times N \times C_{out}}$ is computed using Equation 2.

Subsequently, the $h_{ccm}^{iter}(i)$ for the i -th shadow manifold of the web service time series is obtained using Equation 3. Since each testing iteration involves multiple shadow manifolds, the h_{ccm}^{iter} is calculated as the average of the representations across all shadow manifolds, as defined in Equation 4. While \mathbf{M}_{cc}^{iter} remains constant and is set to \mathbf{M}_{cc} , which is output by the training stage.

4.2 Backbone Time Series Model

The Backbone Time Series Model, denoted as TS_Model , processes the input time series embedding $\mathbf{X} \in \mathbb{R}^{B \times N \times L_x \times C_{in}}$ and outputs a feature representation $h_{ts}^{iter} \in \mathbb{R}^{B \times N \times d_{ts}}$:

$$h_{ts}^{iter} = \text{TS_Model}(\mathbf{X}),$$

which is concatenated with h_{ccm}^{iter} , generated by the CCPlus in training or testing mode, to jointly predict the web service traffic time series.

Based on the baseline evaluation performances across three real-world web service traffic datasets at multiple prediction granularities (Tables 1, 2, 3, and 4) and insights from recent research [33, 45], TimesNet [47] and iTransformer [24] emerge as two strong-performing baselines among state-of-the-art time series models.

TimesNet [47] identifies and utilizes multi-periodicity, decomposing temporal variations into intraperiod and interperiod components. The core module, TimesBlock, adaptively discovers periodicities and extracts features using a parameter-efficient inception block. iTransformer [24] repurposes the Transformer architecture for time series forecasting by applying attention and feed-forward networks on inverted dimensions. It embeds time points as variate tokens, allowing attention to capture multivariate correlations and the feed-forward network to learn nonlinear variate-specific representations.

To broadly verify the effectiveness of the CCPlus (CCM+) module, we integrate it with these two Backbone Time Series Models, resulting in two variant models, e.g., **CCM+iTransformer** and **CCM+TimesNet**.

4.3 Optimization

For convenient combination with the Backbone Time Series Model and to improve generalization, the CCPlus representation h_{ccm}^{iter} is concatenated with the Time Series Model feature representation

h_{ts}^{iter} . In general, the whole procedure can be formalized as follows:

$$\hat{t} = \text{MLP}\left(h_{ccm}^{iter} \mid h_{ts}^{iter}\right),$$

$$\text{MSE Loss} = \frac{1}{B \cdot N \cdot L_{pred}} \sum_{b=1}^B \sum_{n=1}^N \sum_{l=1}^{L_{pred}} (t_{b,n,l} - \hat{t}_{b,n,l})^2, \quad (5)$$

where $h_{ts}^{iter} \in \mathbb{R}^{B \times N \times d_{ts}}$, and both the ground truth t and predicted values $\hat{t} \in \mathbb{R}^{B \times N \times L_{pred}}$. B represents the batch size, N denotes the number of web services within each batch, d_{ts} refers to the representation dimension of the Backbone Time Series Models, and L_{pred} specifies the prediction length of the web services in the time series.

5 EXPERIMENTS

5.1 Datasets

We conduct experiments on three publicly available real-world web service traffic datasets from Alibaba Group², Microsoft Azure³, and Ant Group⁴. The Ant Group Traffic dataset includes 113 web services spanning a time range of 146 days. The Microsoft Azure Traffic dataset consists of 1,000 web services with a time range of 14 days. Similarly, the Alibaba Group Traffic dataset contains 1,000 web services, covering a total duration of 13 days. The datasets utilized in this study are available at: https://github.com/*****.

5.2 Experiment Settings

5.2.1 Baselines. We evaluate our methods against the following baselines:

- **Large Language Models:** Llama3 [41] and TimeLLM [19].
- **Specialized Web Service Traffic Prediction Models:** MagicScaler [29] and OptScaler [52].
- **General Time Series Prediction Models:** TimesNet [47], TimeMixer [44], and iTransformer [24].

These baselines represent the SOTA approaches in their respective categories. Unlike these baselines, which ignore causal relationships among web services, our CCPlus module explicitly incorporates them, enhancing feature representations and improving web service traffic prediction performance.

5.2.2 Evaluation Metrics. We evaluate model performances using Mean Squared Error (MSE) and Mean Absolute Error (MAE):

$$\text{MSE} = \frac{1}{k} \sum_{i=1}^k (y_i - \hat{y}_i)^2, \quad \text{MAE} = \frac{1}{k} \sum_{i=1}^k |y_i - \hat{y}_i|,$$

where y_i and \hat{y}_i denote the true and predicted values, respectively, and k is the number of test samples in the test set.

5.2.3 Implementation Details. The implementation uses PyTorch 2.4.0 with random seeds {0, 2, 4}. Llama3 (8B) is fine-tuned using LoRA (rank 16, $\alpha = 32$). The momentum value m is 0.5. The batch size B is 8, $C_{in} = 16$, $\tau_w = 100$, and the Adam optimizer is configured with a learning rate of 0.000001. The input length L_x is 168, and the prediction length L_{pred} is 1. Training is performed on an H100 GPU with $C_{out} = 32$ and $\tau = [1, 2, 3, 4]$. The model is trained for

15 epochs with an early stopping patience of 5 epochs based on validation performance.

5.2.4 Research Questions. The following research questions are investigated: 1) What are the overall performances and prediction accuracies of the models across different granularities? (Section 5.3) 2) How does the CCPlus module impact prediction performance? (Section 5.4) 3) How does evaluation speed vary across methods? (Section 5.5) 4) How do the methods perform under varying hyperparameter settings? (Section 5.6)

5.3 Prediction Performance Analysis

Performance Comparisons. To evaluate the performance of CCPlus (CCM+), we compare two variants of our proposed framework, CCM+TimesNet and CCM+iTransformer, against the baselines introduced in Section 5.2.1. As shown in Table 1, we report the prediction results on three datasets, with the prediction granularity set to 30 minutes. Among all the baselines, Llama3 performs the worst. While large language models have demonstrated effectiveness in reasoning over sequential data, web traffic exhibits significantly higher volatility, posing substantial challenges for plain LLMs to accurately forecast future values. In contrast, TimeLLM inherently treats time series patches as tokens and employs task-specific prompt embeddings for forecasting. Although it captures patch correlations, it still underperforms on dynamic web traffic data compared to methods specifically tailored for time series analysis. MagicScaler and OptScaler, in particular, are designed for service workload prediction. While these models account for the volatility inherent in traffic time series, they fail to explicitly capture the underlying seasonal and trend components, which are crucial for predicting web service traffic driven by human behavior.

TimeMixer addresses this limitation by decomposing time series into seasonal and trend components across multiple periodicities, enabling it to learn decomposed temporal patterns ranging from fine-grained to macro-level perspectives. As a result, TimeMixer achieves superior prediction performance compared to both LLM-based methods and specialized workload prediction models. TimesNet leverages Fourier transforms to derive more adaptive periodicity terms, further reducing prediction errors. On the other hand, iTransformer treats independent time series as tokens, learning both temporal and cross-dimensional correlations by modeling token sequences, and achieves performance comparable to TimesNet. However, all the above methods focus solely on internal temporal patterns while neglecting external causal relationships across multiple time series. To address this limitation, we integrate CCPlus with TimesNet and iTransformer—the two best-performing baseline models—to create two new variants. As observed, while TimesNet and iTransformer employ carefully designed architectures and achieve SOTA performance across different prediction granularity, integrating CCPlus leads to further improvements. This highlights the importance of capturing the causality inherent in web service traffic for accurate traffic volume prediction. Furthermore, CCPlus effectively models this causality, contributing to enhanced predictive performance.

Prediction Granularity Analysis. Prediction granularity is an important factor for traffic forecasting. To assess this, we vary the time interval of each data point in the time series in {1, 5, 15,

²<https://github.com/alibaba/clusterdata/blob/master/cluster-trace-microservices-v2022>

³<https://github.com/Azure/AzurePublicDataset/tree/master>

⁴https://huggingface.co/datasets/kashif/App_Flow/viewer/

Table 1: Average testing performance over three runs with a 30 minutes time interval across three datasets: Alibaba Group Traffic (124,000 test samples), Azure Traffic (134,000 test samples), and Ant Group Traffic (158,313 test samples).

30 Minutes	Alibaba Group Traffic		Microsoft Azure Traffic		Ant Group Traffic		Overall Mean	
Method	MSE	MAE	MSE	MAE	MSE	MAE	MSE	MAE
MagicScaler [29]	3.4909	0.5362	42.0655	0.8441	1.5513	1.0743	15.7026	0.8182
OptScaler [52]	3.5708	0.6147	33.7485	0.9459	1.3017	0.9421	12.8737	0.8342
Llama3 [41]	7.0570	1.1545	43.8206	1.8958	3.4346	1.5931	18.1041	1.5478
TimeLLM [19]	3.4985	0.5339	17.2852	0.7088	1.5049	1.0560	7.4295	0.7662
TimeMixer [44]	3.1429	0.5455	15.1801	0.6759	1.4036	0.9950	6.5755	0.7388
iTransformer [24]	3.1247	0.5428	19.5574	0.7933	1.4116	1.0010	8.0312	0.7790
CCM+iTransformer (ours)	3.0773	0.5098 ↓6.08%	14.3191 ↓26.8%	0.6482 ↓18.3%	1.3162	0.9402	6.2375	0.6994
TimesNet [47]	3.1843	0.5406	16.6185	0.7177	1.4096	0.9989	7.0708	0.7524
CCM+TimesNet (ours)	3.0206 ↓5.14%	0.5200 ↓3.81%	14.9237 ↓10.2%	0.6791 ↓5.4%	1.2897 ↓8.51%	0.9350 ↓6.40%	6.4113	0.7114

Table 2: Average testing performance over three runs with a 15 minutes time interval across three datasets: Alibaba Group Traffic (249,000 test samples), Azure Traffic (268,000 test samples), and Ant Group Traffic (316,739 test samples).

15 Minutes	Alibaba Group Traffic		Microsoft Azure Traffic		Ant Group Traffic		Overall Mean	
Method	MSE	MAE	MSE	MAE	MSE	MAE	MSE	MAE
MagicScaler [29]	3.3695	0.5262	19.2405	0.6764	1.5044	1.0544	8.0381	0.7523
OptScaler [52]	3.4188	0.5950	17.0180	0.7560	1.3069	0.9503	7.2479	0.7671
Llama3 [41]	7.4170	1.1452	12.6471	1.5288	3.3408	1.5700	7.8016	1.4147
TimeLLM [19]	3.3954	0.5242	6.7723	0.6217	1.5176	1.0579	3.8951	0.7346
TimeMixer [44]	2.8915	0.5004	5.8507	0.5522	1.3962	0.9900	3.3795	0.6809
iTransformer [24]	2.8854	0.5118	5.7501	0.5310	1.4017	0.9938	3.3457	0.6789
CCM+iTransformer (ours)	2.8374	0.4932	5.0156	0.4582	1.3127	0.9368	3.0552	0.6294
TimesNet [47]	2.8635	0.4904	5.0550	0.4641	1.3962	0.9876	3.1049	0.6474
CCM+TimesNet (ours)	2.7151 ↓5.18%	0.4823 ↓1.65%	4.7434 ↓6.16%	0.4422 ↓4.72%	1.2951 ↓7.24%	0.9199 ↓6.85%	2.9179	0.6148

Table 3: Average testing performance over three runs with a 5 minutes time interval across three datasets: Alibaba Group Traffic (748,000 test samples), Azure Traffic (806,000 test samples), and Ant Group Traffic (950,217 test samples).

5 Minutes	Alibaba Group Traffic		Microsoft Azure Traffic		Ant Group Traffic		Overall Mean	
Method	MSE	MAE	MSE	MAE	MSE	MAE	MSE	MAE
MagicScaler [29]	3.2469	0.5176	9.3378	0.5473	1.5326	1.0640	4.7058	0.7096
OptScaler [52]	3.1070	0.4862	8.5807	0.5410	1.3214	0.9373	4.3364	0.6548
Llama3 [41]	7.3436	1.1474	11.5244	1.3587	3.3047	1.5606	7.3909	1.3556
TimeLLM [19]	3.2588	0.5071	6.5393	0.5063	1.4974	1.0459	3.7652	0.6864
TimeMixer [44]	2.7051	0.4818	3.0460	0.3890	1.3923	0.9819	2.3811	0.6176
iTransformer [24]	2.6458	0.4664	3.0367	0.3769	1.3939	0.9853	2.3588	0.6095
CCM+iTransformer (ours)	2.5657	0.4460	2.9780	0.3662	1.3025	0.9398	2.2821	0.5840
TimesNet [47]	2.1681	0.3925	2.8696	0.3527	1.3923	0.9822	2.1433	0.5758
CCM+TimesNet (ours)	1.8103 ↓16.50%	0.3394 ↓13.53%	2.6347 ↓8.19%	0.3150 ↓10.69%	1.2871 ↓7.56%	0.9287 ↓5.45%	1.9107	0.5277

30} minutes and compare the model performances in Table 1, 2, 3 and 4. Note that the more fine-grained time interval setting would generate more data samples as reported in the table caption. First, we observe that CCMPlus consistently improves the SOTA models (TimesNet and iTransformer), underscoring the importance of considering causality among service traffic patterns. Notably, CCMPlus demonstrates flexibility in integrating with various SOTA backbone models, highlighting its potential for performance enhancement. Second, the performance improvements diminish for the 1-minute prediction granularity setting. This is because service traffic is highly dynamic and volatile, and fine-grained time series data often lack a sufficient time duration to accumulate information necessary for capturing reliable causal relationships. Nevertheless, CCMPlus

still achieves the best performance, further demonstrating its superiority in extracting hidden causal relationships and boosting prediction accuracy even under challenging conditions.

5.4 Ablation Study

CCM+TimesNet consistently outperforms multiple baselines across three datasets. Using CCM+TimesNet, we conduct an ablation study on the most challenging dataset, Microsoft Azure Traffic. Table 5 presents the impact of individual modules in CCM+TimesNet, yielding the following insights: (1) Removing the CCMPlus module (w/o CCMPlus) degrades model performance, as CCMPlus generates feature representations that capture causal relationships among web services, enhancing traffic prediction accuracy. (2) Excluding the Backbone Time Series Model (w/o Backbone Time Series Model)

Table 4: Average testing performance over three runs with a 1 minute time interval across three datasets: Alibaba Group Traffic (3,744,000 test samples), Azure Traffic (4,032,000 test samples), and Ant Group Traffic (4,751,424 test samples).

1 Minute	Alibaba Group Traffic		Microsoft Azure Traffic		Ant Group Traffic		Overall Mean	
Method	MSE	MAE	MSE	MAE	MSE	MAE	MSE	MAE
MagicScaler [29]	2.7799	0.4783	6.7159	0.4748	1.9403	1.1674	3.8120	0.7068
OptScaler [52]	3.2586	0.4912	6.5052	0.4693	1.3629	0.9598	3.7089	0.6401
Llama3 [41]	7.6830	1.1101	7.8901	0.6657	3.2022	1.5345	6.2584	1.1034
TimeLLM [19]	3.1173	0.4423	5.3406	0.4513	1.4188	1.0059	3.2922	0.6332
TimeMixer [44]	2.6458	0.4664	2.4406	0.3253	1.3918	0.9800	2.1594	0.5906
iTransformer [24]	2.3571	0.2800	2.3565	0.2875	1.3918	0.9804	2.0351	0.5160
CCM+iTransformer (ours)	2.3677	0.2776	2.3206	0.2782	1.3608	0.9618	2.0164	0.5059
TimesNet [47]	2.2003	0.2609	2.2419	0.2602	1.3917	0.9791	1.9446	0.5001
CCM+TimesNet (ours)	2.1979 ↓ 0.11%	0.2612	2.2503	0.2573 ↓ 1.09%	1.3344 ↓ 4.12%	0.9520 ↓ 2.77%	1.9275	0.4902

Table 5: Ablation study on the Microsoft Azure Traffic dataset with a 5 minutes time interval, including 806,000 test samples.

Method	MSE	MAE
CCM+TimesNet (ours)	2.6347	0.3150
w/o CCMPPlus	2.8696	0.3527
w/o Backbone Time Series Model	2.9981	0.3627

Table 6: Evaluation speed of various methods on the Microsoft Azure Traffic dataset with a 5 minutes time interval, tested on an H100 device. All methods use the same evaluation batch size.

Method	Parameter Volume	Evaluation Speed
Llama3	8 Billion	18.2221s/batch
TimeLLM	7 Billion	92.0710s/batch
MagicScaler	111220	0.0072s/batch
OptScaler	22608	0.0067s/batch
TimeMixer	267578	0.0069s/batch
iTransformer	22626	0.0038s/batch
CCM+iTransformer (ours)	252241	0.0064s/batch
TimesNet	2375283	0.4638s/batch
CCM+TimesNet (ours)	2604898	0.5045s/batch

also reduces performance. The deep learning-based backbone extracts essential seasonal and trend-related temporal features, which are crucial for accurate web service traffic forecasting.

5.5 Evaluation Speed

As shown in Table 6, large language model (LLM)-based methods generally exhibit slower evaluation speeds due to their substantial parameter volumes. In contrast, our methods, CCM+TimesNet and CCM+iTransformer, achieve relatively fast evaluation speeds while outperforming other baselines, as demonstrated in Tables 1, 2, 3, and 4. Overall, the CCMPPlus module enhances prediction performance while maintaining a reasonable computational efficiency.

Table 7: Hyperparameter analysis of momentum value m for causal correlation matrix, conducted on the Microsoft Azure Traffic dataset with a 5 minutes time interval using the CCM+TimesNet method. The dataset comprises 806,000 test samples, and the results are averaged over three experiments.

m	MSE	MAE
0	2.6346 82873	0.3150 20664
0.2	2.6346 82146	0.3150 20501
0.5 (ours)	2.6346 80012	0.3150 20010
0.8	2.6346 79774	0.3150 20189

5.6 Hyperparameter Configuration

Tables 7 and 8 present the hyperparameter analysis, evaluating the impact of the following parameters:

C_{in} defines the embedding dimension of the input time series \hat{X} . As shown in Table 8, the model maintains stable performance across values, demonstrating robustness. Increasing this dimension enhances feature richness, but for efficiency, we set $C_{in} = 16$.

C_{out} defines the embedding dimension of shadow manifold points. A small value may miss features, while a large one can introduce noise. To balance representation quality and efficiency, we set $C_{out} = 32$.

The values in τ define the dilation parameter in Conv1D, controlling the number of shadow manifolds. Increasing this number enhances feature extraction but incurs higher computational costs. To balance accuracy and efficiency, we set $\tau = [1, 2, 3, 4]$.

As shown in Table 8, momentum value m stabilizes the causal correlation matrix by integrating current and past iterations, as defined in Equation 1. Setting m loses general features, while $m = 0.8$ reduces adaptability. We choose $m = 0.5$ for a balance between stability and adaptability.

5.7 Case Study

Using the Azure Traffic dataset, we compute causal relationships between web services with the CCMPPlus module. To visualize, we compare Service A with twenty randomly sampled services and plot the causal correlation heatmap (Figure 9), where Service A exhibits a strong causal correlation with the third service, referred to as

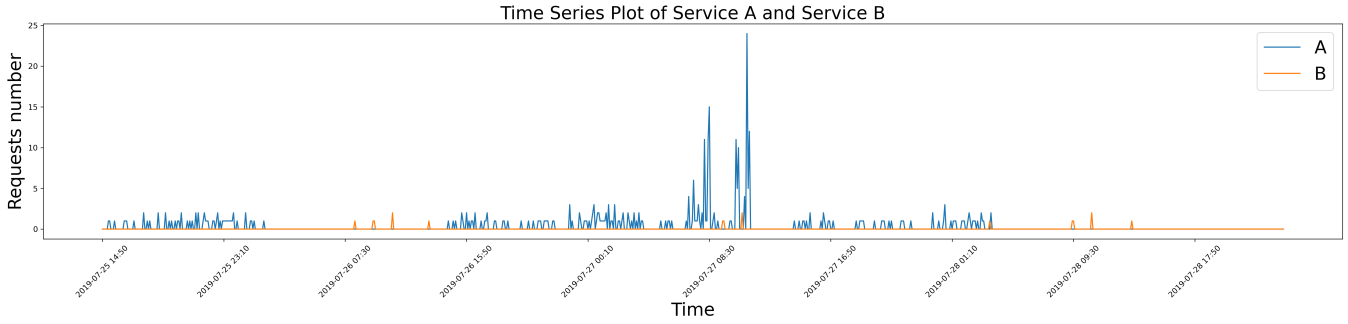


Figure 8: The causal relationship between web service A and service B

Table 8: Hyperparameter analysis of C_{in} , C_{out} , and τ , conducted on the Microsoft Azure Traffic dataset with a 5 minutes time interval using the CCM+TimesNet. The dataset comprises 806,000 test samples, and the results are averaged over three experiments.

C_{in}	MSE	MAE	C_{out}	MSE	MAE	τ	MSE	MAE
12	2.6873	0.3178	28	2.8307	0.3149	[1, 2, 3]	2.7945	0.3157
14	2.8256	0.3385	30	2.6894	0.3223	[1, 2, 3, 4] (ours)	2.6347	0.3150
16 (ours)	2.6347	0.3150	32 (ours)	2.6347	0.3150	[1, 2, 3, 4, 5]	2.6531	0.3144
18	2.7078	0.3170	34	2.6357	0.3143			
20	2.6311	0.3117	36	2.7461	0.3273			



Figure 9: The causal relationship with regard to Web service A in the heatmap.

Service B. To further analyze this relationship, we plot the traffic time series of Services A and B over the same period (Figure 8). The inverse correlation—when one service’s request volume rises, the other’s declines—confirms the strong causal relationship observed in the heatmap.

6 CONCLUSION

Inspired by causality in ecology, we propose the CCMPlus module, which captures causal relationships between web services and integrates with time series models to improve web service traffic prediction.

CCMPlus first constructs shadow manifolds for each web service time series. It then estimates each time point of target time series

using points from the shadow manifolds of other web services. By comparing these estimations with the ground truth of the target time series, a causal correlation matrix is computed, quantifying inter-service causal dependencies. The causal matrix is then applied to the shadow manifold embeddings, generating the CCMPlus representation, which encodes causal relationships. This representation is concatenated with the time series model’s output, bridging the gap in causal inference and enhancing prediction performance.

We evaluate CCMPlus-integrated models on real-world web service traffic datasets from Alibaba Group, Microsoft Azure, and Ant Group. The results demonstrate that CCMPlus consistently improves web service traffic prediction, confirming its effectiveness.

REFERENCES

- [1] 1996. State space reconstruction parameters in the analysis of chaotic time series—the role of the time window length. *Physica D: Nonlinear Phenomena* 95, 1 (1996), 13–28.
- [2] Khadejah Al-talak and Onytra Abbass. 2021. Detecting Server-Side Request Forgery (SSRF) Attack by using Deep Learning Techniques. *International Journal of Advanced Computer Science and Applications* 12, 12 (2021). <https://doi.org/10.14569/IJACSA.2021.0121230>
- [3] Saleha Alharthi, Afra Alshamsi, Anoud Alseieri, and Abdulmalik Alwarafy. 2024. Auto-Scaling Techniques in Cloud Computing: Issues and Research Directions. *Sensors* 24, 17 (2024), 5551.
- [4] Marta Catillo, Umberto Villano, and Massimiliano Rak. 2023. A survey on auto-scaling: how to exploit cloud elasticity. *International Journal of Grid and Utility Computing* 14, 1 (2023), 37–50.
- [5] Peng Chen, Yingying ZHANG, Yunyao Cheng, Yang Shu, Yihang Wang, Qingsong Wen, Bin Yang, and Chenjuan Guo. [n.d.]. Pathformer: Multi-scale Transformers with Adaptive Pathways for Time Series Forecasting. In *The Twelfth International Conference on Learning Representations*.
- [6] Mustafa Daraghme, Suhil Bani Melhem, Anjali Agarwal, Nishith Goel, and Marzia Zaman. 2018. Linear and logistic regression based monitoring for resource management in cloud networks. In *2018 IEEE 6th international conference on future internet of things and cloud (FiCloud)*. IEEE, 259–266.
- [7] Abhimanyu Das, Weihao Kong, Andrew Leach, Shaan K Mathur, Rajat Sen, and Rose Yu. [n.d.]. Long-term Forecasting with TiDE: Time-series Dense Encoder.

- Transactions on Machine Learning Research* ([n. d.]).
- [8] Jinliang Deng, Xiushi Chen, Renhe Jiang, Du Yin, Yi Yang, Xuan Song, and Ivor W. Tsang. 2024. Disentangling Structured Components: Towards Adaptive, Interpretable and Scalable Time Series Forecasting. *IEEE Transactions on Knowledge & Data Engineering* 36, 08 (Aug. 2024), 3783–3800. <https://doi.org/10.1109/TKDE.2024.3371931>
 - [9] Hatice Vildan Dudukcu, Murat Taskiran, Zehra Gulru Cam Taskiran, and Tulay Yildirim. 2023. Temporal Convolutional Networks with RNN approach for chaotic time series prediction. *Applied soft computing* 133 (2023), 109945.
 - [10] Jean-Yves Franceschi, Aymeric Dieuleveut, and Martin Jaggi. 2019. Unsupervised scalable representation learning for multivariate time series. *Advances in neural information processing systems* 32 (2019).
 - [11] Yanghu Guo and Wenbin Yao. 2018. Applying gated recurrent units approaches for workload prediction. In *NOMS 2018-2018 IEEE/IFIP Network Operations and Management Symposium*. IEEE, 1–6.
 - [12] Kaiming He, Haoqi Fan, Yuxin Wu, Saining Xie, and Ross Girshick. 2020. Momentum contrast for unsupervised visual representation learning. In *Proceedings of the IEEE/CVF conference on computer vision and pattern recognition*. 9729–9738.
 - [13] Pradeep Hewage, Ardhendu Behera, Marcello Trovati, Ella Pereira, Morteza Ghahremani, Francesco Palmieri, and Yonghui Liu. 2020. Temporal convolutional neural (TCN) network for an effective weather forecasting using time-series data from the local weather station. *Soft Computing* 24 (2020), 16453–16482.
 - [14] Yazhou Hu, Bo Deng, and Fuyang Peng. 2016. Autoscaling prediction models for cloud resource provisioning. In *2016 2nd IEEE International Conference on Computer and Communications (ICCC)*. IEEE, 1364–1369.
 - [15] Zhigang Hu, Hui Kang, and Meiguang Zheng. 2019. Stream data load prediction for resource scaling using online support vector regression. *Algorithms* 12, 2 (2019), 37.
 - [16] RJ Hyndman. 2018. *Forecasting: principles and practice*. OTexts.
 - [17] Manar Bani Issa, Mustafa Daraghmeh, Yaser Jararweh, Mahmoud Al-Ayyoub, Mohammad Alsmirat, and Elhadj Benkhelifa. 2017. Using logistic regression to improve virtual machines management in cloud computing systems. In *2017 IEEE 14th International Conference on Mobile Ad Hoc and Sensor Systems (MASS)*. IEEE, 628–635.
 - [18] Lina Ji and Jie Xiong. 2022. Superprocesses for the Population of Rabbits on Grassland. *Proceedings of the Steklov Institute of Mathematics* 316, 1 (2022), 195–208.
 - [19] Ming Jin, Shiyu Wang, Lintao Ma, Zhixuan Chu, James Y Zhang, Xiaoming Shi, Pin-Yu Chen, Yuxuan Liang, Yuan-Fang Li, Shirui Pan, et al. [n.d.]. Time-LLM: Time Series Forecasting by Reprogramming Large Language Models. In *The Twelfth International Conference on Learning Representations*.
 - [20] Deepak Kapgate. 2014. Weighted moving average forecast model based prediction service broker algorithm for cloud computing. *International Journal of Computer Science and Mobile Computing* 3, 2 (2014), 71–79.
 - [21] Anoop S Kumar and Somnath Mazumdar. 2016. Forecasting HPC workload using ARMA models and SSA. In *2016 International conference on information technology (ICIT)*. IEEE, 294–297.
 - [22] Suraj Kumar, Soumi Chattopadhyay, and Chandranath Adak. 2024. TPMCF: Temporal QoS Prediction using Multi-Source Collaborative Features. *IEEE Transactions on Network and Service Management* (2024).
 - [23] Haoyu Liao, Tong-yu Liu, Jianmei Guo, Bo Huang, Dingyu Yang, and Jonathan Ding. 2024. Retrospecting Available CPU Resources: SMT-Aware Scheduling to Prevent SLA Violations in Data Centers. *IEEE Transactions on Parallel & Distributed Systems* 01 (2024), 1–17.
 - [24] Yong Liu, Tengge Hu, Haoran Zhang, Haixu Wu, Shiyu Wang, Lintao Ma, and Mingsheng Long. [n.d.]. iTransformer: Inverted Transformers Are Effective for Time Series Forecasting. In *The Twelfth International Conference on Learning Representations*.
 - [25] Alberto Martin-Lopez. 2020. AI-driven web API testing. In *Proceedings of the ACM/IEEE 42nd international conference on software engineering: companion proceedings*. 202–205.
 - [26] Katerina Mitropoulou, Panagiotis Kokkinos, Polyzois Soumplis, and Emmanouel Varvarigos. 2024. Anomaly detection in cloud computing using knowledge graph embedding and machine learning mechanisms. *Journal of Grid Computing* 22, 1 (2024), 6.
 - [27] Kin G Olivares, Cristian Challu, Grzegorz Marcjasz, Rafal Weron, and Artur Dubrawski. 2023. Neural basis expansion analysis with exogenous variables: Forecasting electricity prices with NBEATSx. *International Journal of Forecasting* 39, 2 (2023), 884–900.
 - [28] Boris N Oreshkin, Dmitri Carpov, Nicolas Chapados, and Yoshua Bengio. [n.d.]. N-BEATS: Neural basis expansion analysis for interpretable time series forecasting. In *International Conference on Learning Representations*.
 - [29] Zhicheng Pan, Yihang Wang, Yingying Zhang, Sean Bin Yang, Yunyao Cheng, Peng Chen, Chenjuan Guo, Qingsong Wen, Xiduo Tian, Yunliang Dou, et al. 2023. Magicscaler: Uncertainty-aware, predictive autoscaling. *Proceedings of the VLDB Endowment* 16, 12 (2023), 3808–3821.
 - [30] Anna Pavlenko, Joyce Cahoon, Yiwen Zhu, Brian Kroth, Michael Nelson, Andrew Carter, David Liao, Travis Wright, Jesús Camacho-Rodríguez, and Karla Saur. 2024. Vertically Autoscaling Monolithic Applications with CaasPER: Scalable C container-a s-a-S ervice P erformance E nhanced R esizing Algorithm for the Cloud. In *Companion of the 2024 International Conference on Management of Data*. 241–254.
 - [31] Hong Peng, Xin Xiong, Min Wu, Jun Wang, Qian Yang, David Orellana-Martín, and Mario J Pérez-Jiménez. 2024. Reservoir computing models based on spiking neural P systems for time series classification. *Neural Networks* 169 (2024), 274–281.
 - [32] Wenkang Qi, Jieqian Yao, Jialun Li, and Weigang Wu. 2022. Performer: A Resource Demand Forecasting Method for Data Centers. In *International Conference on Green, Pervasive, and Cloud Computing*. Springer, 204–214.
 - [33] Xiangfei Qiu, Jilin Hu, Lekui Zhou, Xingjian Wu, Junyang Du, Buang Zhang, Chenjuan Guo, Aoying Zhou, Christian S. Jensen, Zhenli Sheng, and Bin Yang. 2024. TFB: Towards Comprehensive and Fair Benchmarking of Time Series Forecasting Methods. *Proc. VLDB Endow* 17, 9 (2024), 2363–2377.
 - [34] Li Ruan, Yu Bai, Shaoning Li, Shuibing He, and Limin Xiao. 2023. Workload time series prediction in storage systems: a deep learning based approach. *Cluster Computing* (2023), 1–11.
 - [35] JT Sean and J Taylor. 2018. Forecasting at scale. *Am. Stat* 72, 1 (2018), 37–45.
 - [36] Meng Shen, Zehui Tan, Dusit Niyato, Yuzhi Liu, Jiawen Kang, Zehui Xiong, Liewang Zhu, Wei Wang, and Xuemin Shen. 2024. Artificial Intelligence for Web 3.0: A Comprehensive Survey. *Comput. Surveys* 56, 10 (2024), 1–39.
 - [37] Martin Straesser, Stefan Geissler, Stanislav Lange, Lukas Kilian Schumann, Tobias Hossfeld, and Samuel Kounev. 2025. Trust your local scaler: A continuous, decentralized approach to autoscaling. *Performance Evaluation* 167 (2025), 102452.
 - [38] George Sugihara, Robert May, Hao Ye, Chih-hao Hsieh, Ethan Deyle, Michael Fogarty, and Stephan Munch. 2012. Detecting causality in complex ecosystems. *science* 338, 6106 (2012), 496–500.
 - [39] Mingtian Tan, Mike A Merrill, Vinayak Gupta, Tim Althoff, and Thomas Hartvigsen. [n.d.]. Are language models actually useful for time series forecasting?. In *The Thirty-eighth Annual Conference on Neural Information Processing Systems*.
 - [40] Chang Tian, Matthew B. Blaschko, Wenpeng Yin, Mingzhe Xing, Yinliang Yue, and Marie-Francine Moens. 2024. A Generic Method for Fine-grained Category Discovery in Natural Language Texts. In *Proceedings of the 2024 Conference on Empirical Methods in Natural Language Processing*, Yaser Al-Onaizan, Mohit Bansal, and Yun-Nung Chen (Eds.). Association for Computational Linguistics, Miami, Florida, USA, 3548–3566. <https://doi.org/10.18653/v1/2024.emnlp-main.208>
 - [41] Hugo Touvron, Thibaut Lavril, Gautier Izacard, Xavier Martinet, Marie-Anne Lachaux, Timothée Lacroix, Baptiste Rozière, Naman Goyal, Eric Hambro, Faisal Azhar, et al. 2023. Llama: Open and efficient foundation language models. *arXiv preprint arXiv:2302.13971* (2023).
 - [42] A Vaswani. 2017. Attention is all you need. *Advances in Neural Information Processing Systems* (2017).
 - [43] Huiqiang Wang, Jian Peng, Feihu Huang, Jince Wang, Junhui Chen, and Yifei Xiao. 2023. Micn: Multi-scale local and global context modeling for long-term series forecasting. In *The eleventh international conference on learning representations*.
 - [44] Shiyu Wang, Haixu Wu, Xiaoming Shi, Tengge Hu, Huakun Luo, Lintao Ma, James Y Zhang, and JUN ZHOU. [n.d.]. TimeMixer: Decomposable Multiscale Mixing for Time Series Forecasting. In *The Twelfth International Conference on Learning Representations*.
 - [45] Yuxuan Wang, Haixu Wu, Jiayang Dong, Yong Liu, Mingsheng Long, and Jianmin Wang. 2024. Deep time series models: A comprehensive survey and benchmark. *arXiv preprint arXiv:2407.13278* (2024).
 - [46] Yuxuan Wang, Haixu Wu, Jiayang Dong, Guo Qin, Haoran Zhang, Yong Liu, Yunzhong Qiu, Jianmin Wang, and Mingsheng Long. 2024. Timexer: Empowering transformers for time series forecasting with exogenous variables. *arXiv preprint arXiv:2402.19072* (2024).
 - [47] Haixu Wu, Tengge Hu, Yong Liu, Hang Zhou, Jianmin Wang, and Mingsheng Long. [n.d.]. TimesNet: Temporal 2D-Variation Modeling for General Time Series Analysis. In *The Eleventh International Conference on Learning Representations*.
 - [48] Haixu Wu, Jiehui Xu, Jianmin Wang, and Mingsheng Long. 2021. Autoformer: Decomposition transformers with auto-correlation for long-term series forecasting. *Advances in neural information processing systems* 34 (2021), 22419–22430.
 - [49] Ailing Zeng, Muxi Chen, Lei Zhang, and Qiang Xu. 2023. Are transformers effective for time series forecasting?. In *Proceedings of the AAAI conference on artificial intelligence*, Vol. 37. 11121–11128.
 - [50] Yunhao Zhang and Junchi Yan. 2023. Crossformer: Transformer utilizing cross-dimension dependency for multivariate time series forecasting. In *The eleventh international conference on learning representations*.
 - [51] Tian Zhou, Ziqing Ma, Qingsong Wen, Xue Wang, Liang Sun, and Rong Jin. 2022. Fedformer: Frequency enhanced decomposed transformer for long-term series forecasting. In *International conference on machine learning*. PMLR, 27268–27286.
 - [52] Ding Zou, Wei Lu, Zhibo Zhu, Xingyu Lu, Jun Zhou, Xiaojin Wang, Kangyu Liu, Kefan Wang, Renen Sun, and Haiqing Wang. 2024. OptScaler: A Collaborative Framework for Robust Autoscaling in the Cloud. *Proceedings of the VLDB Endowment* 17, 12 (2024), 4090–4103.